Geochimica et Cosmochimica Acta 375 (2024) 217–228

Contents lists available at ScienceDirect

Geochimica et Cosmochimica Acta

journal homepage: www.elsevier.com/locate/gca

Continental subduction controls regional magma heterogeneity and distribution of porphyry deposits in post-collisional settings

Christian G. Soder[a,b,*], Jerry Dunga[c], Rolf L. Romer[d]

[a] Institut für Geowissenschaften, Universität Heidelberg, Im Neuenheimer Feld 234–236, 69120 Heidelberg, Germany
[b] Institut für Mineralogie und Kristallchemie, Universität Stuttgart, Azenbergstr. 18, 70174 Stuttgart, Germany
[c] Earth Sciences Division, University of Papua New Guinea, Port Moresby 134, Papua New Guinea
[d] Deutsches GeoForschungsZentrum GFZ, Telegrafenberg, 14473 Potsdam, Germany

ARTICLE INFO

Associate editor: Weidong Sun

Keywords:
Ultrapotassic rocks
Continental subduction
Post-collisional magmatism
Porphyry Cu-Au deposits
Papua New Guinea

ABSTRACT

Continental subduction is the major cause of regional heterogeneities in the lithospheric mantle and contrasting types of magmatism and mineralization in post-collisional settings. We illustrate the relation between the nature of the subducted crust and the character of magmatism for the Late Miocene New Guinea Orogen that formed by the collision of the Australian continental margin with an island arc. The bipartite nature of the subducted Australian plate margin, with Precambrian crust in the west and Phanerozoic accreted arcs in the east, is reflected in the contrasting magmatism along the strike of the New Guinea Orogen. The chemical signature of the subducted crust is particularly prominent in small-volume Late Miocene–Quaternary ultrapotassic rocks of New Guinea. In the west, ultrapotassic lavas have low εNd values (−12.6 to −20.9), indicating the recycling of ancient continental material. Conversely, high εNd values of +3.5 to +4.5 are found in ultrapotassic lavas from eastern New Guinea. This suggests recycling of juvenile continental material, similar to the orthogneisses exposed in the Late Miocene ultrahigh-pressure metamorphic complex of the D'Entrecasteaux Islands. By comparison with ultrapotassic rocks from other orogenic belts, we show that crustal recycling is responsible for regionally contrasting redox conditions in the lithospheric mantle, which may explain why porphyry-type deposits are important in some regions but absent in others.

1. Introduction

Mantle-derived magmas in post-collisional settings are typically potassium-rich and characterized by high contributions of recycled continental material. This is related to the melting of metasomatized mantle formed during an earlier stage of subduction. Particularly during continental collision, continental input to the subduction zone can increase significantly, resulting in a regionally heterogeneous lithospheric mantle. The composition of the subducted material introduces a variety of metasomatic reaction products (e.g., Avanzinelli et al., 2009; Mallik et al., 2015; Condamine et al., 2016; Gülmez et al., 2023) and affects the oxidation state of the mantle (e.g., Mungall, 2002; Richards and Şengör, 2017; Cannaò and Malaspina, 2018).

Some of the largest porphyry copper–gold deposits are bound to K-rich igneous rocks and have formed in post-collisional settings (e.g., Müller and Groves, 1993; Sillitoe, 2002; Hou et al., 2009; Richards, 2009; Grondahl and Zajacz, 2017; Zhang and Audétat, 2017; Chang and Audétat, 2023a). Such deposits are concentrated in a few well-endowed regions (e.g., Richards, 2009, 2015a). The reason for this restricted spatial distribution is poorly understood and may be related to both the oxidation state and metal content of the mantle source. Oxidizing conditions are generally considered essential for the mobilization of chalcophile elements during mantle melting and their enrichment during melt evolution (e.g., Sillitoe, 2010; Audétat and Simon, 2012; Sun et al., 2013; Park et al., 2021; Richards, 2022; Rielli et al., 2022). Consequently, the nature of the subducted crustal material may account for regional differences in ore potential.

Post-collisional melting of subduction-modified lithospheric mantle produces associations of calc-alkaline, shoshonitic, and ultrapotassic rocks. These co-magmatic suites can be explained by variable degrees of partial melting of a common mantle source (e.g., Foley, 1992; Conticelli et al., 2009; Soder and Romer, 2018). Incipient, low-degree melting produces ultrapotassic magmas with largest contributions of recycled continental material (e.g., Prelević et al., 2008; Conticelli et al., 2009;

* Corresponding author at: Institut für Geowissenschaften, Universität Heidelberg, Im Neuenheimer Feld 234–236, 69120 Heidelberg, Germany.
E-mail address: christian.soder@mailbox.org (C.G. Soder).

https://doi.org/10.1016/j.gca.2024.04.015
Received 1 July 2023; Accepted 9 April 2024
Available online 12 April 2024

Zhao et al., 2009). Their geochemical compositions, especially their trace element and Sr-Nd-Pb isotopic signatures, closely reflect that of the regional crust as exposed in local ultrahigh-pressure (UHP) metamorphic complexes (Soder and Romer, 2018). Therefore, ultrapotassic rocks are ideal for tracing regional differences in the composition of recycled crust, and for addressing the role of recycled material in the formation of post-collisional porphyry deposits.

The plate boundary zone between the Australian and Pacific plates of New Guinea is particularly well suited to study the relation between the nature of subducted continental crust, the oxidation state of the lithospheric mantle, and ore formation. The New Guinea Orogen formed during Late Miocene arc-continent collision (e.g., Cloos et al., 2005; Davies, 2012; Baldwin et al., 2012; Holm et al., 2015) and hosts world-class porphyry Cu-Au deposits (e.g., Cooke et al., 2005). Fundamentally different rocks have been subducted along the strike of the orogen. In the western part, the subducted crust includes Proterozoic rocks of the North Australian Craton. In the eastern part, the continental crust is composed of more juvenile accreted Paleozoic terranes (Hill and Hall, 2003) and rift-related volcanic rocks (Zirakparvar et al., 2013), as exposed in Earth's youngest UHP complex on the D'Entrecasteaux Islands of Papua New Guinea. Ultrapotassic volcanic rocks have been previously described for western New Guinea (Housh and McMahon, 2000) and are newly identified for the eastern segment of the plate boundary zone, where they erupted in the mountains of the Central Range. We characterize regional differences in the nature of the subducted material based on the geochemical signatures of these lavas. By comparing our results with literature data for other collision belts, we demonstrate that the subducted material exerts a strong control on the oxidation state of the local lithospheric mantle and consequently on the regional distribution of post-collisional porphyry deposits.

2. Geological setting

The island of New Guinea is located on the northern margin of the Australian continent and hosts a major orogenic belt. The Central Range, the spine of the island, formed when the Australian passive margin entered a north-dipping subduction zone beneath an island arc during the Miocene (e.g., Hill and Raza, 1999; Hill and Hall, 2003; Cloos et al., 2005; Baldwin et al., 2012; Davies, 2012; Holm et al., 2015). The topography of New Guinea reflects its tectonic subdivision, with a lowland stable platform to the south, an east–west trending fold belt in the center, and a mobile belt to the north (Fig. 1). The platform has a bipartite division along the Tasman Line, which separates the cratonic areas to the west from the areas dominated by Paleozoic and Mesozoic accretionary orogens to the east (Hill and Hall, 2003). West of the Tasman Line, the Proterozoic basement is covered by Cambrian to Devonian and Permian sedimentary rocks. To the east, Early Triassic and older rocks form a low-grade metamorphic basement. From the Jurassic onward, the western and eastern parts of New Guinea have a common sedimentary record (Hill and Hall, 2003; Cloos et al., 2005; Holm et al., 2015). The fold-and-thrust belt, which includes the same rocks as the platform, began to develop in the Late Miocene following arc-continent collision (Hill and Hall, 2003). The Mobile Belt includes Mesozoic to Paleocene ophiolites, distal Mesozoic–Tertiary sediments, medium- to high-grade metamorphic rocks, and abundant Late Oligocene to predominantly Miocene (ca. 20–10 Ma) volcanic and intrusive igneous rocks, known as the Maramuni Arc (Hill and Hall, 2003).

The southwest Pacific has a complex tectonic history. The tectonic setting of the New Guinea Orogen, particularly the orientation and number of subduction zones, remains controversial. Most models favor northward subduction of oceanic crust north of Australia, followed by collision of the Australian margin with an island arc in the Middle Miocene (e.g., Hill and Hall, 2003; Cloos et al., 2005; Holm et al., 2015). Due to the contrasting nature of the basement at the former Australian

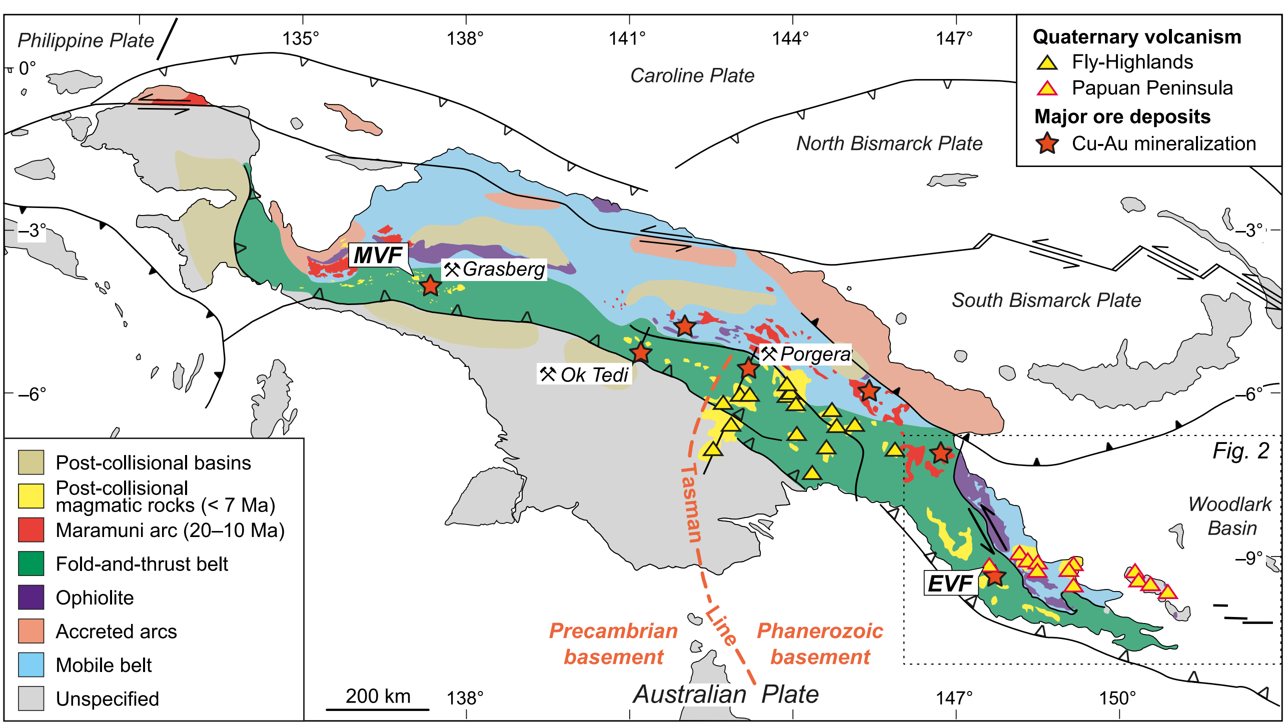

Fig. 1. Map of the New Guinea region showing major geological features of the collisional orogen (compiled from Hill and Hall, 2003; Cloos et al., 2005; Davies, 2012; Baldwin et al., 2012). Post-collisional magmatism started at ~7 Ma and is concentrated along the fold-and-thrust belt. Major copper and gold deposits formed during this phase of magmatism. Quaternary volcanic activity is restricted to the Papuan Peninsula (including the D'Entrecasteaux Islands) and the Fly-Highlands Volcanic Provinces. Ultrapotassic volcanic fields are present in western New Guinea (Minjauh Volcanic Field, MVF) and on the Papuan Peninsula of eastern New Guinea (Efogi Volcanic Field, EVF).

passive margin, the subduction zones transported chemically and isotopically distinct continental material into the mantle. Following arc-continent collision, magmatism migrated southward into the fold-and-thrust belt, forming intrusive and volcanic rocks since the Late Miocene (<7 Ma). Some of the world's largest porphyry copper–gold deposits are associated with this post-collisional phase of igneous activity (e.g., Hill et al., 2002; Pollard et al., 2005; Cooke et al., 2005; van Dongen et al., 2010a; Large et al., 2018).

Post-collisional igneous rocks are heterogeneously distributed along the orogen (Fig. 1) and are characterized by considerable compositional variability. The Minjauh Volcanic Field (MVF) in the west, for instance, erupted calc-alkaline, shoshonitic and ultrapotassic lavas at 3–7 Ma (Housh and McMahon, 2000; McMahon, 2001). Major porphyry copper–gold deposits are associated with shallow level intrusions and include the Grasberg and Ok Tedi intrusive complexes, with emplacement ages of 3.4–2.6 Ma and 1.4–1.1 Ma, respectively (e.g., Pollard et al., 2005, 2021; van Dongen et al., 2010a; Large et al., 2018). These intrusions have high-K calc-alkaline and shoshonitic compositions. The largest deposits are positioned west of the Tasman Line. Intrusion-related ore deposits are also present to the east, although they are smaller and less significant (e.g., Holm et al., 2019). Granitic–monzonitic stocks intruded the Suckling-Dayman Massif of the Papuan Peninsula between ~3.7 and ~2.0 Ma (Österle et al., 2020). The Miocene magmatic activity on the Papuan Peninsula has been linked to south-directed subduction of the oceanic Solomon Sea crust at the Trobriand Trough between ~6 and ~2 Ma (Davies et al., 1984; Holm et al., 2016). However, a link between southward subduction of the Solomon Sea plate and high-K magmatism is unlikely, and subduction signatures have been interpreted as inherited from an earlier phase of subduction (Österle et al., 2020).

The eastern segment of the orogenic belt is characterized by two prominent volcanic provinces, the Fly-Highlands and the Papuan Peninsula Volcanic Provinces (Fig. 2), which formed mostly during the Quaternary. The lavas have calc-alkaline to shoshonitic compositions with subduction-related geochemical signatures (e.g., Mackenzie, 1976; Smith, 1982, 2014; Zhang et al., 2015; Misztela et al., 2022). Both volcanic provinces are not related to active subduction, but resulted from remelting of previously subduction-modified mantle (Johnson et al., 1978; Smith, 1982) and are therefore part of the post-collisional magmatic activity.

The Fly-Highlands Province is located within the fold-and-thrust belt to the east of the Tasman Line (Fig. 1). The volcanic province is constituted of several large Quaternary basaltic–andesitic stratovolcanoes (Mackenzie, 1976; Misztela et al., 2022). Volcanic activity started in the late Pliocene or early Pleistocene in response to an episode of tectonic uplift (e.g., Mackenzie, 1976), presumably during lithospheric extension.

The Papuan Peninsula Volcanic Province includes several active volcanic centers (Fig. 2). Mantle melting is a response to extensional tectonics related to the westward propagation of seafloor spreading in the adjoining Woodlark Basin (e.g., Eilon et al., 2015; Jin et al., 2015; Abers et al., 2016). Seafloor spreading in the Woodlark Basin commenced at about 6 Ma (Taylor et al., 1999). This rifting is associated with a low-velocity structure in the upper mantle, reflecting thinned mantle lithosphere, which can be traced for >250 km from the E–W axis of the rift into the extended continent (Eilon et al., 2015). This extensional setting is responsible for the rapid exhumation of Earth's youngest UHP metamorphic complex on the D'Entrecasteaux Islands, with 5–6 M.y. old coesite-bearing eclogites (e.g., Baldwin et al., 2004, 2008; DesOrmeau et al., 2017). The D'Entrecasteaux Islands host active volcanic centers erupting calc-alkaline basalts to highly differentiated peralkaline rhyolites (e.g., Smith, 2014) above significantly thinned mantle lithosphere (Abers et al., 2002). Thicker lithospheric mantle is still available for melting beneath other parts of the collision belt (Abers et al., 2002; Eilon et al., 2015), where smaller volcanic centers are characterized by K-rich primary compositions. For example, primitive shoshonitic pyroclastics erupted at the Waiowa Crater (Baker, 1946). This small volcano formed in 1943–1944 and is located on the Mai'iu Fault, along which rapid exhumation of low-grade, high-*P/T* metamorphic rocks of the Suckling-Dayman metamorphic core complex takes place (e.g., Davies, 1980; Little et al., 2019). Ultrapotassic lavas erupted at the small Quaternary Efogi Volcanic Field (EVF), which represents the

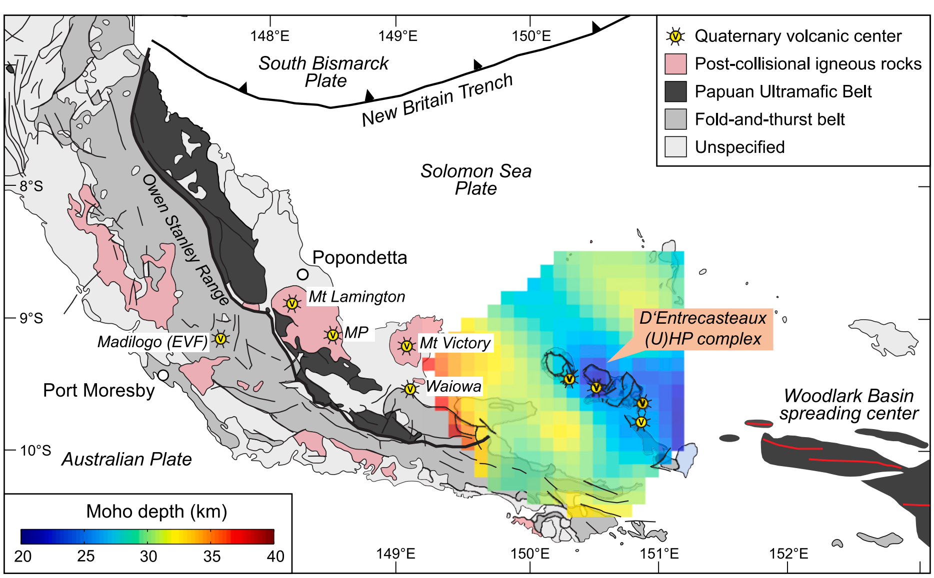

Fig. 2. Simplified geological map of the Papuan Peninsula (after Baldwin et al., 2004) showing the Quaternary eruptive centers of the Papuan Peninsula Volcanic Province, including the Efogi Volcanic Field (EVF) with the Madilogo cinder cone (this study). Mount Lamington stratovolcano erupted violently in 1951 (Taylor, 1958), Mount Victory has erupted historically, and Waiowa volcano formed in 1943–1944 (Baker, 1946). There are several smaller volcanic centers on the Managalase Plateau (MP). Volcanic centers also exist on the D'Entrecasteaux Islands, where Pliocene ultrahigh-pressure (UHP) metamorphic rocks of continental origin are exhumed in a core complex. Active seafloor spreading takes place further east in the Woodlark Basin. Due to the westward progradation of the spreading system, the continental crust and lithospheric mantle beneath the D'Entrecasteaux Islands and adjacent Collingwood Bay are undergoing significant extension, as shown in the color-coded model of crustal thickness (Moho depth) derived from receiver function analysis (Jin et al., 2015). Beneath the D'Entrecasteaux Islands, the lithospheric mantle is being almost completely replaced by asthenospheric mantle (Abers et al., 2002; Eilon et al., 2015).

westernmost extension of the Papuan Peninsula Volcanic Province (Fig. 2).

The Efogi Volcanic Field is located on the southwestern flank of the Owen Stanley Range and consists of small, scattered lava flows erupted in valleys at an elevation of ~700–1250 m above sea level. The lava flows have smooth, flat surfaces, are up to 60 m thick, and rest unconformably on a greenschist-facies metamorphic basement composed of schists, phyllites, and subordinate metavolcanics (Pieters, 1978). The remnant of a small Late Quaternary cinder cone is present at the village of Madilogo along the Naoro River (Blake, 1976). The rocks of the EVF are of primary ultrapotassic composition. Ultrapotassic magmatism has not been previously reported for the eastern part of New Guinea (Papua New Guinea), but is probably more widespread, as indicated by biotite lamprophyre dykes reported for the Musa River area west of Mount Suckling (Green, 1961), and likely contributes to post-collisional magmatism along the entire Central Range.

3. Analytical methods

Mineral and glass compositions were analyzed using a CAMECA SX51 and a CAMECA SX100 electron microprobe at Heidelberg University and the University of Stuttgart, respectively. Phlogopite, leucite and glass were analyzed with a defocused beam (10 μm) at 15 kV acceleration voltage and 10nA beam current. All other minerals were analyzed with a focused beam at 15 kV acceleration voltage and 15nA beam current. Peak counting times were 10 s for K and Na, 20 s for other major elements, and 40 s for minor elements (V, Ni, Zn, Zr, Ba). Background counting times were half the peak counting times on each side of the peak, or the peak-counting times if measured on one side only. Synthetic and natural minerals, glasses, and pure oxides were used for calibration. Raw data were corrected using the 'PAP' procedure provided by CAMECA.

For whole-rock analysis, samples were processed in a steel jaw crusher and powdered in an agate mill. Major elements were determined by wavelength-dispersive X-ray fluorescence spectrometry (XRF) on lithium borate fusion disks using a Bruker AXS S8 instrument at Terrachem GmbH, Mannheim, Germany. International reference samples were used for calibration. Loss on ignition (LOI) was determined by heating of 2 g of sample powder at 1050 °C for 8 h. Trace element analyses were performed at GeoZentrum Nordbayern (GZN), University of Erlangen-Nuremberg, using an Agilent 7500i ICP-MS, equipped with an Analyte Excite 193 nm ArF excimer laser ablation system (Teledyne Photon Machines). Measurements were performed on the lithium borate fusion disks at four ablation lines of 50 μm diameter. The SiO_2 concentrations from the XRF analysis were used as internal standards and the NIST SRM 612 glass reference material was used for external calibration. Further details on the accuracy and reproducibility of the mineral and whole-rock analysis and the analyses of international reference materials are provided in Supplementary Tables S1 and S2.

Measurements of Sr, Nd and Pb isotopic compositions were performed at the Deutsches GeoForschungsZentrum (GFZ), Potsdam, using splits of the powders used for whole-rock analysis. Samples were digested in concentrated HF on a hot plate for four days, dried down, taken up in 2 M HNO_3 to convert fluorides to nitrates, slowly dried down again, and redissolved in 6 M HCl. The clear solutions were aliquoted for isotope analysis. Strontium, Nd and Pb were separated using standard ion-exchange procedures (e.g., Romer et al., 2005 and references therein). The Sr and Nd isotopic compositions were measured using a Thermo-Fischer-Scientific (TFS) Triton thermal ionization multicollector mass spectrometer (TIMS) operated in dynamic multicollection mode, using single Ta-filaments and double Re-filaments, respectively. Strontium and Nd isotope ratios were normalized to $^{86}Sr/^{88}Sr = 0.1194$ and $^{146}Nd/^{144}Nd = 0.7219$, respectively. Lead was loaded on single Re-filaments and its isotopic composition was measured using a TFS Triton TIMS operated in static mode. Instrumental fractionation was corrected by 0.1 % per a.m.u. as determined from the long-term reproducibility of Pb reference material NBS-981. The accuracy and precision of the reported Pb isotope ratios are better than 0.1 % at a 2σ level of uncertainty.

4. Samples and results

Pristine volcanic rock samples were collected from the Efogi Volcanic Field (EVF). The lavas have porphyritic textures and contain up to 2 mm large phenocrysts of olivine with euhedral inclusions of Cr-spinel and laths of marginally resorbed phlogopite. Clinopyroxene and subordinate apatite form microphenocrysts. Some samples also contain microphenocrysts of leucite, which also forms rims around resorbed phlogopite. The matrix consists of a feldspathic mesostasis or, more rarely, of fresh glass containing abundant euhedral microphenocrysts of leucite. Accessory armalcolite-pseudobrookite and titanomagnetite form euhedral crystals in the matrix. Photomicrographs and backscattered electron images are shown in Supplementary Figs. S1 and S2.

All samples are ultrapotassic with K_2O of 5.0–7.3 wt% and K_2O/Na_2O of 2.8–4.6 at high MgO concentrations of >8 wt% and SiO_2 concentrations of 50.8–52.9 wt%. Two samples with olivine accumulation have slightly lower SiO_2 and higher MgO (Fig. 3). Despite high alkalinity, the samples are metaluminous rather than peralkaline (molar ratio of $(K_2O + Na_2O)/Al_2O_3 < 1$).

The trace element patterns (Fig. 4) show a general light rare earth element (LREE) enrichment with chondrite-normalized La_N/Yb_N of 14–30 and weak, variable Eu anomalies with Eu/Eu* ($=Eu_N/(Sm_N \times Gd_N)^{0.5}$) of 1.14–0.83. Primitive mantle-normalized element abundance patterns are characterized by enrichments in large ion lithophile elements, positive Pb anomalies, and negative anomalies in Nb and Ta, with no significant negative Ti anomalies. Strong positive anomalies are present in Sr, Zr and Hf (Fig. 4). The samples show small variations in radiogenic Sr-Nd and Pb isotopes (Fig. 5), and typical mantle values with little radiogenic Sr ($^{87}Sr/^{86}Sr = 0.703676$–$0.703882$) and radiogenic Nd ($^{143}Nd/^{144}Nd = 0.512816$–$0.512867$). The Pb isotopic compositions fall above the Northern Hemisphere Reference Line ($^{206}Pb/^{204}Pb$ = 18.787–18.850; $^{207}Pb/^{204}Pb$ = 15.562–15.589; $^{208}Pb/^{204}Pb$ = 38.552–38.665). Whole-rock elemental and isotopic analyses of all samples, along with GPS coordinates of sampling localities, are provided in Supplementary Tables S3–S5.

Mineral and glass compositions were analyzed using EPMA for a scoria sample from the Madilogo cinder cone and a glassy lava from Fagume Creek (a detailed petrological description and mineral formula calculations are provided in Supplementary Text S2 and Tables S6–S12). The mineralogy reflects the undifferentiated nature of the alkali-rich (but metaluminous) and relatively oxidized melts. Abundant euhedral olivine phenocrysts (core compositions with Fo_{91-88}) contain numerous tiny octahedrons of Cr-spinel with high Cr# (=Cr/(Cr + Al) of 0.85–0.76) and phlogopite phenocrysts with up to 2 wt% Cr_2O_3. Olivine rims (Fo_{87-84}) enclose clinopyroxene and apatite, together with less magnesian Cr-spinel. Clinopyroxene is chemically zoned with decreasing Mg and Si toward the rims, and increasing Ti and tetrahedral Al. The Efogi lavas contain significant amounts of Fe^{3+} in early formed Cr-spinel and late Fe-Ti oxides (titanomagnetite and pseudobrookite-armalcolite) as calculated from stoichiometry. Based on mineralogy, the Efogi samples have lamproitic affinities but do not classify as lamproites, as they are not peralkaline. Contrasting to the Efogi ultrapotassic lavas, primary lamproitic minerals show low Al but can contain significant Fe^{3+} in tetrahedral coordination, which is related to the excess of alkalies relative to aluminum in peralkaline liquids. In lamproites *sensu stricto*, higher Cr# of Cr-spinel (with Al_2O_3 typically <6 wt %) and low Al_2O_3 (<0.3 wt%) of pseudobrookite-armalcolite are also likely related to peralkalinity (see Supplementary Text S2 for details).

The overall major and trace element compositions of ultrapotassic lavas from New Guinea are comparable to those of other orogens, such as the Alpine-Himalayan belt (Prelević et al., 2008; Conticelli et al., 2009). Orogenic ultrapotassic rocks show a continuous trend from silica-

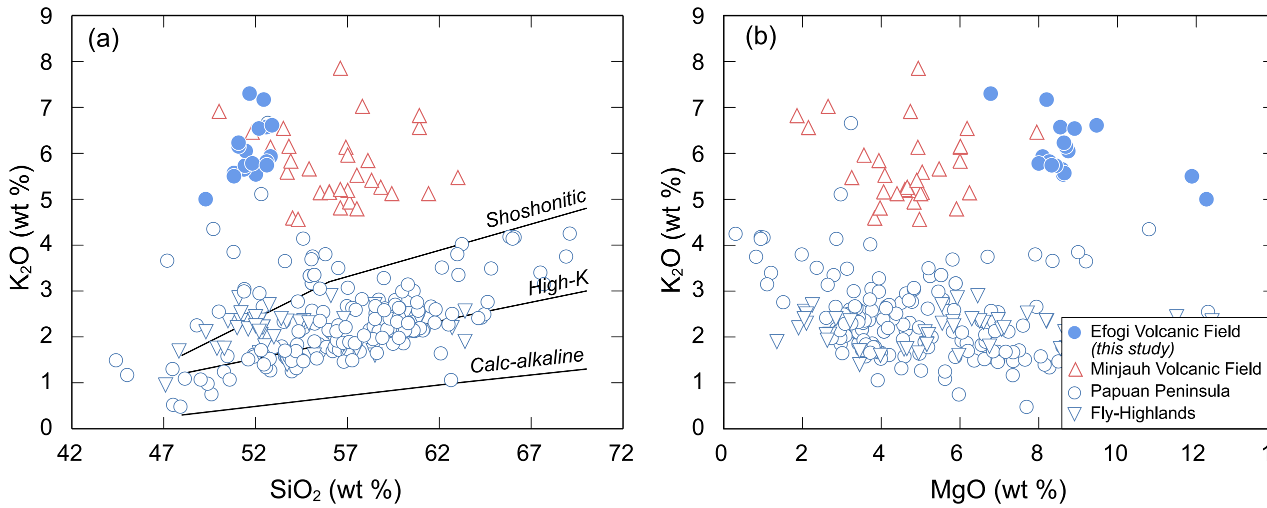

Fig. 3. Ultrapotassic lavas are found in the Efogi Volcanic Field (this study) and the Minjauh Volcanic Field within the New Guinea Orogen (Housh and McMahon, 2000; McMahon, 2001). The large Quaternary volcanoes of Papua New Guinea in the eastern part of the orogen erupted predominantly lavas of calc-alkaline to shoshonitic compositions (for data sources see Supplementary Table S13). Ultrapotassic compositions are defined as K_2O and MgO > 3 wt% with K_2O/Na_2O > 2 according to Foley et al. (1987).

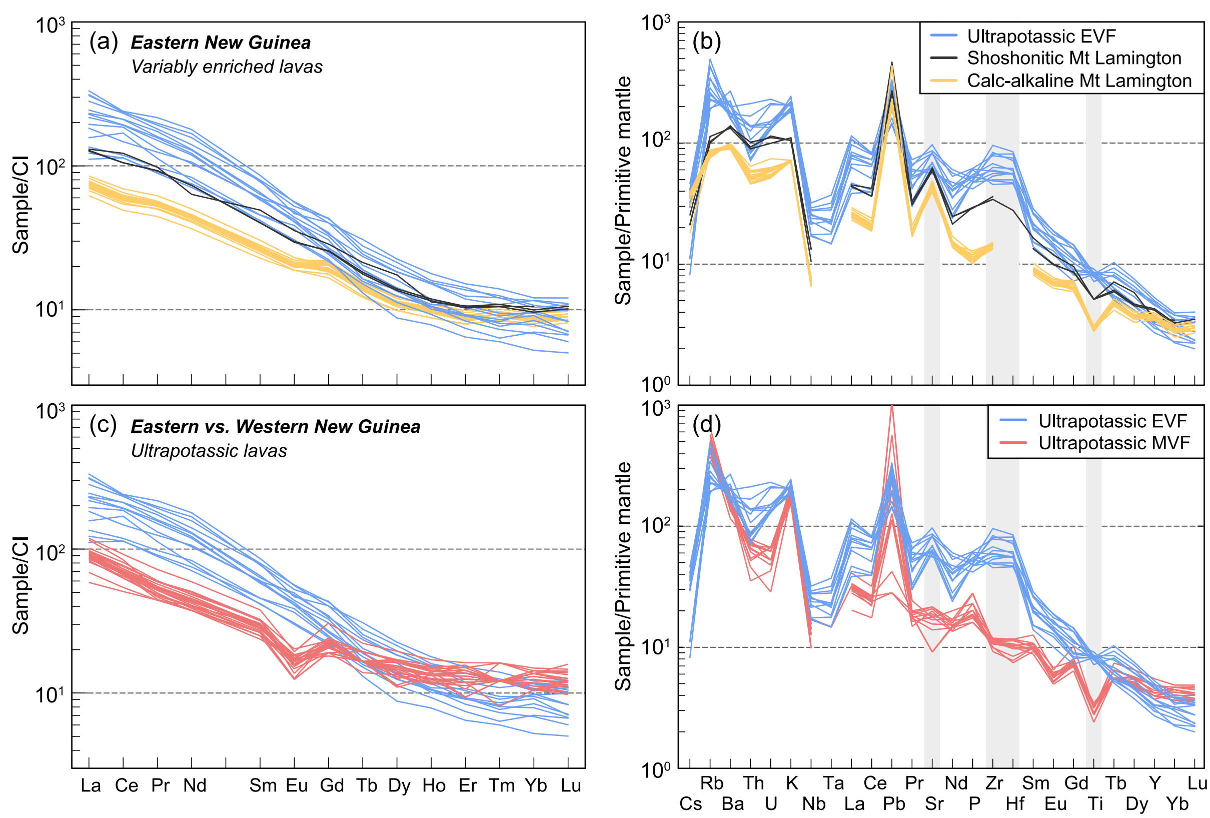

Fig. 4. Comparison of trace element compositions of ultrapotassic lavas from the Efogi Volcanic Field (EVF) with (a, b) less enriched post-collisional shoshonitic and calc-alkaline lavas from eastern New Guinea (Mount Lamington; Zhang et al., 2015) and (c, d) ultrapotassic lavas from western New Guinea (Minjauh Volcanic Field, MVF; McMahon, 2001). Please note that calc-alkaline, shoshonitic, and ultrapotassic lavas from eastern New Guinea display similar patterns. Strikingly different patterns are observed for ultrapotassic rocks from eastern and western New Guinea (e.g., U, Sr, Zr, Eu).

rich lamproites to kamafugites with regionally contrasting compositions. The major element compositions of the New Guinea lavas fall between the lamproitic (high SiO_2 and low Al_2O_3 and CaO) and kamafugitic (low SiO_2 and high CaO) endmembers.

We have applied the oxygen barometer of Ballhaus et al. (1991) to estimate oxygen fugacities of mantle-derived magmas using the compositions of olivine and coexisting Cr-spinel (see Supplementary Text S3 for details). Application to the EVF lavas yields oxygen fugacities around FMQ +1.5, in the range of arc basalts, but higher than values typical of mid-ocean ridge basalts (e.g., Cottrell et al., 2021). We complemented our data with analyses of olivine-spinel pairs from K-rich rock samples from the Mediterranean region of the Alpine-Himalayan belt (see Supplementary Tables S16 and S17 for data sources and results). These rocks record highly variable oxygen fugacities, ranging from more

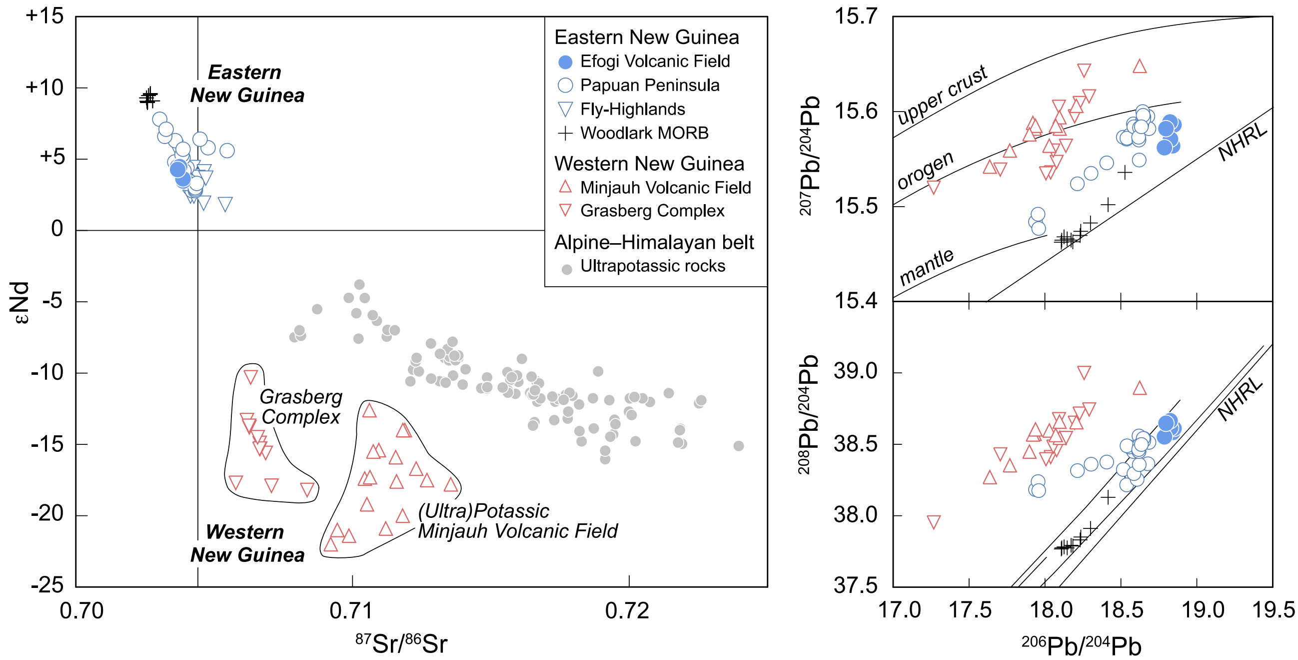

Fig. 5. Post-collisional igneous rocks from eastern and western New Guinea show distinct Sr, Nd and Pb isotopic compositions, with signatures typical of mantle and ancient continental crust, respectively. The dichotomy in the geochemistry of mantle-derived magmas is inherited from the subducted continental crust and reflects the crustal architecture of the Australian continental shelf, which is segmented by the Tasman Line (Fig. 1). Data sources: Grasberg Complex (including the Ertsberg intrusion of the Gunung Bijih mining district), Minjauh Volcanic Field (Housh and McMahon, 2000), Fly-Highlands (Hamilton et al., 1983), Papuan Peninsula (Hegner and Smith, 1992; Zhang et al., 2015), and Woodlark MORBs (Park et al., 2018). Data sources for ultrapotassic lavas with silica-rich lamproitic affinity from the Alpine-Himalayan belt (Western Alps, Italy; Tuscany, Italy; Murcia–Almeria, Spain; W Lhasa Block, Tibet) are provided in Supplementary Table S14.

oxidized to significantly reduced compared to arc basalts. Oxygen fugacities vary systematically between different post-collisional provinces.

5. Discussion

5.1. Linking ultrapotassic magmatism with continental subduction in eastern New Guinea

Subduction recycling of continental material produces enriched domains within the subcontinental lithosphere that are more fusible compared to the ambient depleted mantle. Post-collisional formation of K-rich magmas is commonly associated with such metasomatized mantle domains. Orogenic ultrapotassic rocks, therefore, provide valuable insights into these recycling processes, containing high amounts of recycled material. However, ultrapotassic magmatism has rarely been linked to subducted high-pressure lithologies. The New Guinea Orogen is an outstanding site to study this relationship. Quaternary potassium-rich mantle-derived volcanism is associated with strong extensional tectonics, which is also responsible for the rapid exhumation of the Earth's youngest UHP metamorphic complex on the D'Entrecasteaux Islands (Davies and Warren, 1988; Baldwin et al., 2004, 2008; DesOrmeau et al., 2017). This metamorphic complex provides direct samples of the subducted material, placing constraints on the nature of the subducted crust.

The high-pressure metamorphic rocks are of continental origin and are predominantly composed of felsic and intermediate meta-igneous rocks with Late Cretaceous protolith ages (Davies and Warren, 1988; Zirakparvar et al., 2013). The ultrapotassic magmas of eastern New Guinea have mantle-like ε_{Nd} values (+3.5 to +4.5), that closely match those of the meta-igneous rocks of the metamorphic complex with present-day values of +1.7 to +4.3 (Zirakparvar et al., 2013), as well as their non-metamorphic equivalents, which are represented by the Whitsunday Volcanic Province in NE Queensland, Australia (Zirakparvar et al., 2013) with values of +1.1 to +6.5 (Ewart et al., 1992).

Peak *P-T* conditions of the UHP complex are constrained to 2.7–3.1 GPa and ~715 °C for coesite eclogites (DesOrmeau et al., 2017). The corresponding stable eclogite-facies mineral assemblage for the surrounding gneisses comprises coesite, phengite, K-feldspar, jadeite-rich pyroxene, kyanite, clinozoisite, and subordinate garnet with accessory titanite/rutile (Brownlee et al., 2011). Peak *P-T* conditions are located slightly above the wet granite solidus, where water-fluxing can produce large amounts of hydrous silicate melt (or supercritical fluid). Close to the wet solidus, liquids are alkaline and have highly fractionated K/Na ratios, due to the stability of residual jadeite-rich pyroxene in the felsic rocks (Schmidt et al., 2004). These highly potassic, alkaline liquids efficiently mobilize trace elements to the overlying mantle, resulting in metasomatic reactions or partial melting (e.g., Hermann and Rubatto, 2009).

The Efogi Volcanic Field ultrapotassic lavas of eastern New Guinea have trace element signatures that can be explained by the inheritance from subducted continental crust, i.e., felsic–intermediate calc-alkaline igneous rocks. The non-metamorphic volcanic equivalents in the Whitsunday Volcanic Province consist of dacitic to rhyolitic ignimbrites, with minor intermediate and mafic pyroclastics, lavas and dykes. Magmatism is interpreted to be extension-related, with re-melting of calc-alkaline crust and the addition of basaltic magmas derived from a depleted mantle source (Ewart et al., 1992; Bryan et al., 2000). Recycling of calc-alkaline crust is consistent with positive Pb anomalies and negative Nb-Ta anomalies of the EVF ultrapotassic rocks. Other striking trace element features can be attributed to the evolved character of the subducted protoliths. Prominent positive Zr-Hf anomalies of the EVF lavas further argue for meta-igneous protoliths. Such anomalies develop during amphibole-dominated middle to lower crustal calc-alkaline differentiation (Nandedkar et al., 2016). Amphibole fractionation also explains the observed co-variation between Zr/Nb and Zr/Sm (Fig. 6) or increasing Zr/Nb with roughly decreasing Gd_N/Yb_N (=2.7–4.5). The variability of trace element ratios sensitive to fractional crystallization (Fig. 6) probably reflects recycling of variably evolved or heterogeneous material. Positive Sr anomalies (with Sr/Y of 53–103) and weak Eu anomalies are indicative of intermediate to moderately differentiated (e.g.,

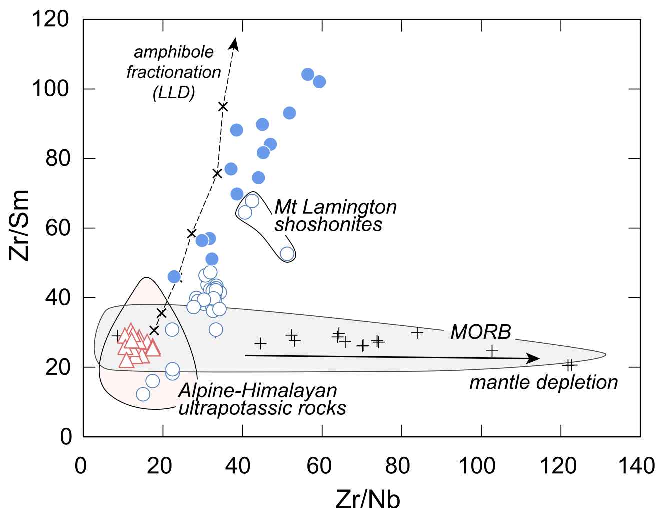

Fig. 6. In the Zr/Sm vs. Zr/Nb diagram, lavas from the Efogi Volcanic Field and from Mount Lamington plot along the experimentally determined mid- to lower crustal calc-alkaline differentiation trend (liquid line of descent, LLD; Nandedkar et al., 2016), likely reflecting the recycling of igneous rocks that were variably affected by amphibole fractionation. In contrast, the ultrapotassic rocks from western New Guinea (MVF) and the Alpine-Himalayan belt (Prelević et al., 2008; Conticelli et al., 2009) are characterized by low Zr/Nb and Zr/Sm ratios. Symbols as in Fig. 5.

rhyodacitic) calc-alkaline magmatic rocks (Nandedkar et al., 2016), as opposed to highly evolved, granitic continental material that would produce strongly negative Eu anomalies accompanied by low Sr/Y, K/Rb and Nb/Ta ratios (Fig. 7; Soder and Romer, 2018).

The example of eastern New Guinea demonstrates the genetic link between ultrapotassic magmatism and continental subduction, and shows that key geochemical features of orogenic ultrapotassic rocks are already established in the early stages of ultrahigh-pressure crustal melting. Ultrapotassic magmas can therefore be used to trace the nature of recycled crust, as they inherit isotopic and trace element patterns from the subducted crust.

5.2. Regional variations of the crustal component in K-rich magmatism of New Guinea

The orogenic range of New Guinea is characterized by sporadic igneous activity since the Miocene (Fig. 1). The igneous rocks are heterogeneously distributed and show compositional variability that may be partly inherited from the mantle source. In western (Indonesian) New Guinea, intermediate magmas intruded the Central Range, such as the Grasberg Igneous Complex. In addition, small volcanic centers such as the Minjauh Volcanic Field (MVF) produced shoshonitic and ultrapotassic lavas (Housh and McMahon, 2000). In eastern New Guinea, the more voluminous Pliocene–Quaternary volcanic activity of the Fly-Highlands and Papuan Peninsula erupted dominantly calc-alkaline to shoshonitic compositions (e.g., Mackenzie, 1976; Zhang et al., 2015; Misztela et al., 2022).

Lavas from the Papuan Peninsula have mantle-like Sr-Nd isotopic compositions comparable to the EVF (Fig. 5). Furthermore, the EVF shares distinct geochemical similarities with the nearby Mount Lamington stratovolcano, such as positive anomalies of Sr, Zr, and Hf (Fig. 4a, b; Zhang et al., 2015). These anomalies become more pronounced with increasing degree of trace element enrichment, i.e., from the calc-alkaline to shoshonitic compositions of Mount Lamington to the ultrapotassic lavas of the EVF (Fig. 4a, b). We interpret these differences to reflect variations in the contributions of metasomatized and depleted lithospheric mantle. The more enriched magmas of the EVF represent incipient, low-degree partial melts of metasomatized mantle, whereas the less enriched magmas result from higher degrees of melting and were therefore more strongly diluted by depleted basaltic melts from ambient peridotite. The degree of melting (and dilution) is related to lithospheric extension, which is particularly strong in eastern New Guinea due to the west-directed propagation of oceanic spreading in the Woodlark Basin (e.g., Eilon et al., 2015), east of the Papuan Peninsula (Fig. 2).

Ultrapotassic rocks in western New Guinea have different geochemical signatures compared to their eastern equivalents (Figs. 4–7). The Late Miocene to Pliocene shoshonitic to ultrapotassic volcanic rocks of the MVF were emplaced near the giant Ertsberg-Grasberg mining district (Housh and McMahon, 2000; McMahon, 2001). The MVF rocks are variably differentiated (Mg# 66.9–43.6). The crustal trace element and isotopic signatures, however, are interpreted to reflect the metasomatized mantle source, rather than being affected by fractional crystallization and assimilation of crustal rocks. Incompatible trace element contents of the MVF lavas are lower compared to the EVF lavas, but still at high levels and, therefore, insensitive to crustal contamination. Furthermore, there is no correlation between indices of differentiation, e.g., SiO_2, and isotopic ratios or trace element ratios used here to characterize the nature of the crustal component.

The MVF rocks lack the characteristic Zr-Hf anomalies (Fig. 4). Negative Eu anomalies, low K/Rb ratios of 153 ± 32 (2SD) and low Sr/Y ratios of 21 ± 16 compared to the EVF lavas (average K/Rb of 301 ± 157 and Sr/Y of 87 ± 28) indicate the recycling of evolved continental material (Soder and Romer, 2018). The MVF ultrapotassic lavas display strongly negative ε_{Nd} values of –12.6 to –20.9 and high $^{208}Pb/^{204}Pb$ for a given $^{206}Pb/^{204}Pb$ value (Fig. 5; Housh and McMahon, 2000). The high $^{208}Pb/^{204}Pb$ values suggest the involvement of material that has experienced ancient loss of Pb and U relative to Th, as is typical for lower crustal rocks (Housh and McMahon, 2000) and deeply weathered sedimentary rocks (Franz et al., 2013). Low ε_{Nd} values also indicate that the enriched domains in the lithospheric mantle sampled by the MVF melts are derived from subducted ancient (Neoproterozoic or Archean) crustal material (Housh and McMahon, 2000), such as the cratons of northern Australia. Precambrian igneous basement and granites derived from Precambrian crustal sources are exposed in the Georgetown and Coen Inliers (Cape York Peninsula, N Australia), bordering New Guinea to the south. These rocks have Sr-Nd isotopic compositions similar to those of the MVF (Black and McCulloch, 1984).

The distribution of post-collisional magmas in New Guinea follows a general, regional pattern in terms of radiogenic isotopes, with ancient signatures in the west and mantle-like signatures in the east. Ancient isotopic signatures are observed for the Grasberg Igneous Complex (Fig. 5). The involvement of ancient continental material is also relevant for the Ok Tedi porphyry copper deposit, where Pleistocene zircon has negative ε_{Hf} values of -6.5 ± 2 (van Dongen et al., 2010a). In contrast, further east, Late Miocene igneous zircon from felsic rocks has mantle-like Hf isotopic compositions of +6 to +7 (Holm et al., 2015). The Quaternary volcanic provinces in the east, the Fly-Highlands and the Papuan Peninsula Volcanic Provinces, have mantle-like Sr-Nd isotopic compositions with no evidence for the involvement of old continental material (Fig. 5). The boundary between the two major lithospheric domains lies between Ok Tedi and the Fly-Highlands Volcanic Province (Fig. 1).

The bipartite distribution of geochemical signatures in post-collisional igneous rocks mirrors the bipartite nature of the neighboring Australian continent. The Tasman Line in Australia separates cratonic areas in the west from the areas dominated by Paleozoic and Mesozoic accretionary orogens in the east, which have experienced recurrent additions of juvenile material during subduction processes affecting eastern Australia (e.g., Rosenbaum, 2018). We argue that Late Miocene continental subduction of the Australian plate in the north-directed subduction zone has contaminated the mantle beneath the entire New Guinea collisional belt. Lithospheric extension, unrelated to this mantle metasomatism, eventually resulted in preferential melting of

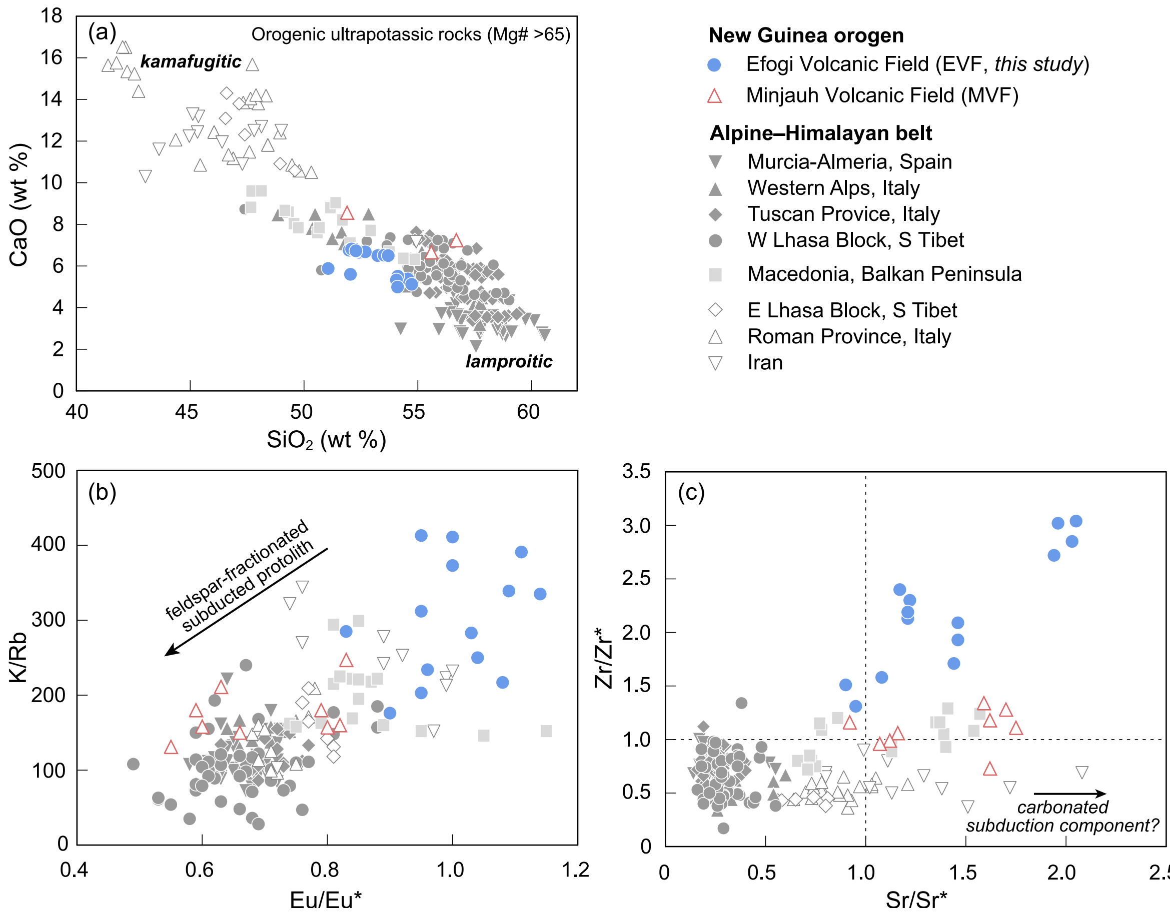

Fig. 7. Comparison of post-collisional ultrapotassic lavas from the New Guinea Orogen with corresponding rocks from the Alpine-Himalayan belt. Major and trace element compositions of undifferentiated ultrapotassic rocks (Mg#>65) are used to characterize the recycled crustal component. (a) In the CaO vs. SiO_2 diagram, orogenic ultrapotassic rocks plot along an array defined by the kamafugite and silica-rich lamproite endmembers. Ultrapotassic lavas from New Guinea have intermediate compositions. Values are normalized to volatile-free compositions. (b) Negative Eu anomalies in primitive rocks reflect recycling of highly differentiated protoliths. The correlation between negative Eu anomalies and K/Rb ratios suggests that K/Rb signatures are also inherited from the protoliths. (c) Negative Sr and Zr-Hf anomalies (expressed as $Sr_N/(Ce_N \times Nd_N)^{0.5}$ and $Zr_N/(Nd_N \times Sm_N)^{0.5}$, respectively) indicate recycling of differentiated crust. Subduction of carbonated sediments may result in positive Sr anomalies, and subduction of evolved (amphibole-fractionated) calc-alkaline igneous protoliths produces positive Sr and Zr-Hf anomalies (see text for details). MVF data are from McMahon (2001). Data sources for Alpine-Himalayan ultrapotassic rocks are given in Supplementary Table S14.

metasomatized mantle and the production of post-collisional magmas.

The mineralized Porgera intrusive complex, emplaced at 6 Ma, represents a geochemical anomaly in the post-collisional magmatic evolution of New Guinea. It has a Na-alkaline composition with a distinct intra-plate geochemical signature (Richards et al., 1990). However, magma production is likely related to the common tectonic process of lithospheric extension, resulting in decompression melting of convecting mantle due to reactivation of older, deep trans-lithospheric structures at the boundary between the two crustal domains. The location of this igneous complex may therefore coincide with the position of the Tasman Line in New Guinea (Fig. 1).

5.3. *Controls of crustal recycling on post-collisional porphyry deposit formation*

Collisional belts worldwide host important porphyry copper deposits associated with post-collisional magmatism, but their spatial distribution is heterogeneous (e.g., Richards, 2015a). Identifying differences in magma formation between mineralized and barren provinces is crucial for understanding metal enrichment in collisional belts. The lithospheric mantle is an important source of ore-forming magmas in post-collisional settings (e.g., Hill et al., 2002; Pettke et al., 2010; Holwell et al., 2019; Grondahl and Zajacz, 2017; Zhang and Audétat, 2017; Rielli et al., 2022; Chang and Audétat, 2023a). Melting under oxidizing conditions is one of the critical parameters, as it allows efficient dissolution of sulfides from the mantle source and further prevents loss of chalcophile elements during subsequent igneous differentiation related to early sulfide saturation (e.g., Sillitoe, 2010; Audétat and Simon, 2012; Sun et al., 2013; Park et al., 2021; Richards, 2022; Rielli et al., 2022). Importantly, the oxidation state of the lithospheric mantle is influenced by subduction recycling of continental material (e.g., Mungall, 2002; Richards and Şengör, 2017, Cannaò and Malaspina, 2018). As discussed above, the nature of the material subducted in collisional orogens is highly variable. Consequently, the oxidation state of the subducted material can vary widely. The oxygen fugacity (fO_2) of metapelites, for instance, ranges from significantly reduced to oxidized values, whereas high-pressure carbonate and calc-silicate rocks have high fO_2 values of FMQ +2 to FMQ +4 (e.g., Cannaò and Malaspina, 2018 and references therein).

Here, we use primary ultrapotassic lavas to evaluate the role of mantle source preconditioning by crustal recycling, because they closely reflect the nature of the subducted material. Mineralization is typically not directly linked to ultrapotassic magmas, but is associated with high-K calc-alkaline and shoshonitic igneous rocks (e.g., Müller and Groves, 1993; Sillitoe, 2002; Richards, 2009). These rocks form co-genetic suites in post-collisional provinces and are related by variable degrees of partial melting of metasomatized mantle (e.g., Foley, 1992; Conticelli et al., 2009; Soder and Romer, 2018). Ultrapotassic rocks therefore sample the same lithospheric mantle as the magmatic rocks that give rise to orogenic porphyry copper–gold deposits. We note that orogenic magmas can have multiple sources, and the presence of inherited zircon in ore-related intrusions argues for direct involvement of crustal material by assimilation and/or crustal melting (e.g., van Dongen et al., 2010a; Large et al., 2018). However, evolved K-rich calc-alkaline orogenic igneous rocks are predominantly derived from lithospheric mantle contaminated by regional crust, accounting for their prominent continental crust-like geochemical signatures (e.g., Couzinié et al., 2016; Moyen et al., 2017; Chang and Audétat, 2023b).

The orogenic belt of New Guinea is particularly rich in Cu-Au mineralization, and world-class porphyry-type mineral deposits are associated with the Grasberg and Ok Tedi intrusive complexes to the west of the Tasman Line (Fig. 1). Ore-related magmas at Grasberg and Ok Tedi have high-K calc-alkaline and shoshonitic compositions (e.g., McMahon, 1994; van Dongen et al., 2010b) and show ancient isotopic signatures, similar to the ultrapotassic rocks west of the Tasman Line (Fig. 5). Mineralizations are also present to the east, although smaller and less important (e.g., Pollard et al., 2005; Holm et al., 2019), with a porphyry-type deposit located in close proximity to the Efogi Volcanic Field (Fig. 1; Dugmore et al., 1996).

East of the Tasman Line, recycling of calc-alkaline material has an oxidizing effect on the average mantle, as evolved subduction-related volcanics are typically characterized by FMQ values of +1 to +2 (Richards, 2015b; Cottrell et al., 2021). The ultrapotassic EVF lavas of eastern New Guinea formed at FMQ values of about +1.5, reflecting the oxidized lithospheric mantle source (Fig. 8a). Oxidized conditions are further supported by the presence of primary anhydrite in less enriched lavas at Mount Lamington (Taylor, 1958; Arculus et al., 1983). While no information is available on the oxygen fugacity of ultrapotassic rocks in the west, the presence of porphyry deposits along the entire orogenic belt suggests an oxidized lithospheric mantle on both sides of the Tasman Line. We argue that these conditions are provided by the recycling of oxidized material.

Different types of ultrapotassic rocks are found along orogenic belts. Orogenic silica-rich lamproites and kamafugites constitute worldwide endmembers, which can be explained by the subduction of evolved continental crust (metagranitic/metapelitic) and carbonated sediments (e.g., marls or calc-silicates), respectively (e.g., Avanzinelli et al., 2009; Ammannati et al., 2016). Oxygen fugacities derived for prominent examples of these rock types along the Tethyan realm display strong systematic variations, as inferred from the compositions of Cr-spinel or pseudobrookite-like Fe-Ti-oxides (Fig. 8). Recycling of evolved continental material (metapelitic or S-type granitic material) is evidenced by characteristic negative Eu anomalies, pronounced negative Sr anomalies, and low Nb/Ta or K/Rb ratios (Soder and Romer, 2018). The associated lamproitic rocks are typically much more reduced compared to arc basalts. In contrast, recycling of carbonate-rich material has an oxidizing effect on the lithospheric mantle and produces CO_2-rich melts with kamafugitic affinity (Fig. 8a).

The regional heterogeneity in the oxidation state of the metasomatized lithospheric mantle, as documented by ultrapotassic magmas, provides a unique opportunity to link the nature of the subducted material with the spatial distribution of mineralization. The Lhasa Block of the India-Asia collision zone in southern Tibet exhibits a pronounced east–west zonation with distinct geochemical signatures recorded in post-collisional magmas (Hou et al., 2015a). Porphyry deposits are absent in the west but important in the east (e.g., Hou et al., 2009, 2015b; Wang et al., 2018; Luo et al., 2022). Ultrapotassic rocks in the west are characterized by recycling of ancient, evolved Indian continental crust and have silica-rich lamproitic affinities (e.g., Ding et al., 2003; Zhao et al., 2009; Fig. 7). The oxidation state of these magmas is poorly known, but may range from values typical of arc rocks (Li et al., 2020) to more reduced compositions below FMQ, as indicated by the presence of armalcolite (Miller et al., 1999; Fig. 8b). Rocks in the east have juvenile isotopic compositions (Xu et al., 2017), which may be related to recycling of continental material with lower average crustal residence age. In the east, ultrapotassic lamprophyres cutting the Gangdese porphyry copper deposits (Xu et al., 2017) have kamafugitic affinities (Fig. 7a), indicating an oxidized mantle source. Other important porphyry Cu deposits are present along the Arabian-Eurasian collision zone in Iran (e.g., Shafiei et al., 2009; Aghazadeh et al., 2015a), where local mantle-derived magmas also exhibit kamafugitic affinities (e.g., Aghazadeh et al., 2015b; Pang et al., 2015). In the Mediterranean region of the Alpine–Himalayan belt, recycling of evolved metagranitic/metapelitic continental material resulted in reduced lamproitic magmas, such as the

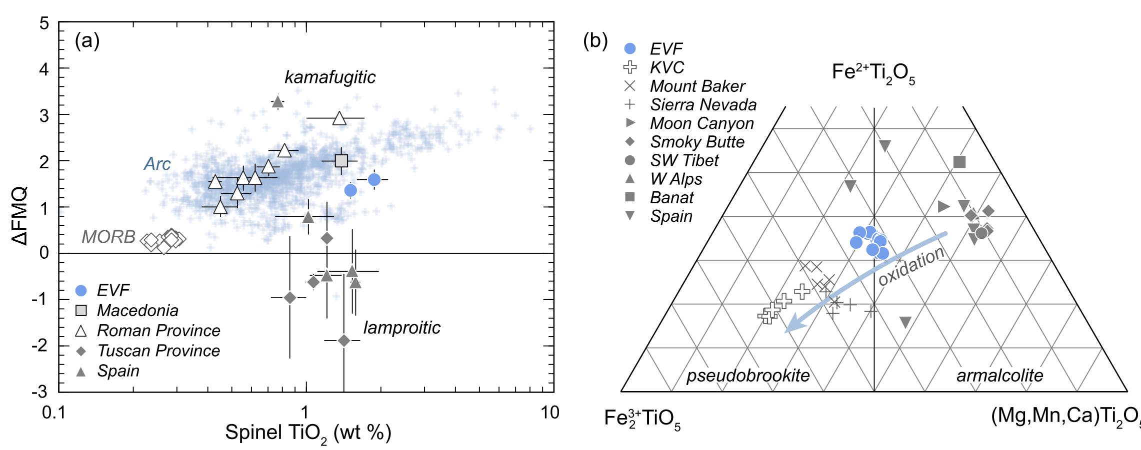

Fig. 8. (a) Orogenic ultrapotassic rocks record highly variable oxygen fugacities, and systematic differences exist between post-collisional provinces. Calculations are based on the $Fe^{3+}/\Sigma Fe$ ratios of Cr-spinel included in olivine using the equation of Ballhaus et al. (1991) and are given relative to FMQ (fayalite-magnetite-quartz buffer). Experimental evidence for reduced conditions of Spanish lamproites was also found by Foley (1985). One oxidized sample from the Spanish province (Jumilla) is anomalous for having a carbonated mantle source (Prelević et al., 2008). Data for arc magmas (Kamchatka) and MORBs are shown for comparison. Error bars are standard deviations of the average of several Cr-spinel-olivine pairs. Further details are provided in Supplementary Text S3. Data sources and results are given in Tables S16 and S17, respectively. (b) Pseudobrookite-like Fe-Ti-Mg oxides are typical accessory phases in ultrapotassic rocks and show variable iron oxidation states. The EVF oxide compositions fall on the boundary between the pseudobrookite and armalcolite compositional fields. Silica-rich lamproitic rocks from the Alpine-Himalayan belt contain armalcolite, indicating reduced conditions. Ultrapotassic lavas from the central Sierra Nevada (California, USA) contain pseudobrookite and record oxidized conditions (Feldstein and Lange, 1999). More rarely, primary pseudobrookite also crystallizes from highly oxidized magmas in volcanic arc settings (>FMQ +2 for a hornblende andesite from Mount Baker, Northern Cascade Arc; Mullen and McCallum, 2013) and from peralkaline rocks in intra-plate settings (e.g., KVC; Katzenbuckel Volcanic Complex, Germany). See Supplementary Table S15 for data sources and Text S2 for further details.

silica-rich lamproites of SE Spain, the lamprophyre dykes of the western Alps, or the ultrapotassic rocks of the Tuscan Magmatic Province, Italy (e.g., Peccerillo, 1999; Prelević et al., 2008; Conticelli et al., 2009; Soder and Romer, 2018). Porphyry Cu deposits are systematically absent in these regions (e.g., Richards, 2015a).

The above examples demonstrate that the production of porphyry-type mineralization is favored in areas where oxidized material is subducted. Recycling of carbonate-bearing material appears to be particularly relevant, but other oxidized lithologies such as calc-alkaline metavolcanics also favor the formation of porphyry copper deposits, as in New Guinea. Conversely, recycling of reduced material effectively prevents the formation of post-collisional porphyry mineralization.

Precious metals may also be contributed directly from the recycled crustal component, as indicated by elevated gold contents recorded in some orogenic K-rich rocks (e.g., Rock and Groves, 1988; Rock et al., 1989). Although elevated ore metal concentrations within the metasomatized mantle are generally not a prerequisite for the production of important ore deposits (e.g., Wang et al., 2020), crustal recycling may contribute to the secondary metal content of porphyry deposits (e.g., Au, Mo), which show regionally contrasting patterns on a global scale (e.g., Sillitoe, 2010).

6. Conclusions

Ultrapotassic volcanism of the New Guinea Orogen is an expression of post-collisional melting of lithospheric mantle. This mantle was metasomatized during the Late Miocene subduction of the Australian passive margin during arc-continent collision. Ultrapotassic rocks in New Guinea form two geochemically contrasting groups. The distribution of these groups is controlled by the Tasman Line, which in Australia marks the boundary between old cratonic areas in the west and young magmatic arcs in the east. Geochemical signatures of K-rich lavas west of the Tasman Line are inherited from ancient crustal material, such as from the cratons of northern Australia. Ultrapotassic lavas east of the Tasman Line have trace element and isotope compositions reflecting those of ultrahigh-pressure gneisses from the D'Entrecasteaux Islands, which have variably differentiated calc-alkaline igneous protoliths. Similar signatures are present in coeval, less enriched shoshonitic and calc-alkaline lavas and are likely inherited from a closely related mantle source.

The contrasting nature of material subducted during collisional processes not only accounts for regional variations in post-collisional magma geochemistry, but may also explain the regional distribution of porphyry copper–gold deposits. The subducted material controls the oxidation state of the metasomatized mantle, which determines whether chalcophile elements can be mobilized and thus whether porphyry-type mineralization can form. Ultrapotassic igneous rocks are ideal tracers of crustal recycling processes in post-collisional magmatic settings, and their oxygen fugacity may be a promising proxy for the chalcophile element fertility of an area.

Data availability

Data are available through heiDATA, an institutional repository for open research data of Heidelberg University, at https://doi.org/10.11588/data/QS478V.

CRediT authorship contribution statement

Christian G. Soder: Conceptualization, Investigation, Visualization, Writing – original draft, Writing – review & editing. **Jerry Dunga:** Investigation, Writing – review & editing. **Rolf L. Romer:** Investigation, Writing – review & editing.

Declaration of competing interest

The authors declare that they have no known competing financial interests or personal relationships that could have appeared to influence the work reported in this paper.

Acknowledgments

The authors thank Helene Brätz (University of Erlangen-Nuremberg), Bettina Hübner (GFZ Potsdam), Thomas Theye (University of Stuttgart), and the late Fredy Rüttimann (Terrachem GmbH, Mannheim) for analytical assistance. We thank Ilona Fin and Oliver Wienand (Heidelberg University) for thin section preparation. The first author especially thanks Hans-Joachim Massonne for fruitful discussions and support during his postdoctoral stay at the University of Stuttgart. Jerry Dunga and Christian Soder are very grateful to the local communities for their permission to collect samples, their support, and their great hospitality during field work in PNG. We thank Weidong Sun for editorial handling, and Dejan Prelević and two anonymous reviewers for constructive comments that improved the quality of the manuscript.

Appendix A. Supplementary material

The supplementary material to this article provides additional information on the methodology and petrology of the samples, as well as details on the calculation of oxygen fugacities (Text S1–S3). In addition, the file contains reference material analyses (Tables S1 and S2) and all research data (Tables S3–S12). The research data include whole-rock analyses (major and trace element concentrations, Sr-Nd-Pb isotope data) and GPS sample locations, as well as electron microprobe data of minerals and glasses from ultrapotassic lavas of the Efogi Volcanic Field. Additional sources of geochemical and mineral chemical data used for comparison in the main article (Tables S13–S16) and results of olivine-spinel oxybarometry (Table S17) are reported. Supplementary material to this article can be found online at https://doi.org/10.1016/j.gca.2024.04.015.

References

Abers, G.A., Ferris, A., Craig, M., Davies, H., Lerner-Lam, A.L., Mutter, L.C., Taylor, B., 2002. Mantle compensation of active metamorphic core complexes at Woodlark rift in Papua New Guinea. Nature 418, 862–865.

Abers, G.A., Eilon, Z., Gaherty, J.B., Jin, G., Kim, Y.H., Obrebski, M., Dieck, C., 2016. Southeast Papuan crustal tectonics: Imaging extension and buoyancy of an active rift. J. Geophys. Res. Solid Earth 121, 951–971.

Aghazadeh, M., Hou, Z., Badrzadeh, Z., Zhou, L., 2015a. Temporal–spatial distribution and tectonic setting of porphyry copper deposits in Iran: constraints from zircon U-Pb and molybdenite Re–Os geochronology. Ore Geol. Rev. 70, 385–406.

Aghazadeh, M., Prelević, D., Badrzadeh, Z., Braschi, E., van den Bogaard, P., Conticelli, S., 2015b. Geochemistry, Sr-Nd-Pb isotopes and geochronology of amphibole- and mica-bearing lamprophyres in northwestern Iran: Implications for mantle wedge heterogeneity in a palaeo-subduction zone. Lithos 216, 352–369.

Ammannati, E., Jacob, D.E., Avanzinelli, R., Foley, S.F., Conticelli, S., 2016. Low Ni olivine in silica-undersaturated ultrapotassic igneous rocks as evidence for carbonate metasomatism in the mantle. Earth Planet. Sci. Lett. 444, 64–74.

Arculus, R.J., Johnson, R.W., Chappell, B.W., McKee, C.O., Sakai, H., 1983. Ophiolite-contaminated andesites, trachybasalts, and cognate inclusions of Mount Lamington, Papua New Guinea: anhydrite-amphibole-bearing lavas and the 1951 cumulodome. J. Volcanol. Geoth. Res. 18, 215–247.

Audétat, A., Simon, A.C., 2012. Magmatic controls on porphyry Cu genesis. In: Hedenquist, J.W., Harris, M., Camus, F. (Eds.), Geology and genesis of major copper deposits and districts of the world: A tribute to Richard Sillitoe. Society of Economic Geologists Special Publication 16, pp. 553–572.

Avanzinelli, R., Lustrino, M., Mattei, M., Melluso, L., Conticelli, S., 2009. Potassic and ultrapotassic magmatism in the circum-Tyrrhenian region: significance of carbonated pelitic vs. pelitic sediment recycling at destructive plate margins. Lithos 113, 213–227.

Baker, G., 1946. Preliminary note on volcanic eruptions in the Goropu Mountains, Southeastern Papua, during the period December 1943, to August 1944. J. Geol. 54, 19–31.

Baldwin, S.L., Monteleone, B.D., Webb, L.E., Fitzgerald, P.G., Grove, M., Hill, E.J., 2004. Pliocene eclogite exhumation at plate tectonic rates in eastern Papua New Guinea. Nature 431, 263–267.

Baldwin, S.L., Webb, L.E., Monteleone, B.D., 2008. Late Miocene coesite-eclogite exhumed in the Woodlark Rift. Geology 36, 735–738.
Baldwin, S.L., Fitzgerald, P.G., Webb, L.E., 2012. Tectonics of the New Guinea region. Annu. Rev. Earth Planet. Sci. 40, 495–520.
Ballhaus, C., Berry, R.F., Green, D.H., 1991. High pressure experimental calibration of the olivine-orthopyroxene-spinel oxygen geobarometer: implications for the oxidation state of the upper mantle. Contrib. Miner. Petrol. 107, 27–40.
Black, L.P., McCulloch, M.T., 1984. Sm-Nd ages of the Arunta, Tennant creek, and Georgetown inliers of Northern Australia. Aust. J. Earth Sci. 31, 49–60.
Blake, D.H., 1976. Madilogo, a late Quaternary volcano near Port Moresby, Papua New Guinea. In: Johnson, R.W. (Ed.), Volcanism in Australasia. Elsevier Sci, Amsterdam, pp. 253–258.
Brownlee, S.J., Hacker, B.R., Salisbury, M., Seward, G., Little, T.A., Baldwin, S.L., Abers, G.A., 2011. Predicted velocity and density structure of the exhuming Papua New Guinea ultrahigh-pressure terrane. J. Geophys. Res. Solid Earth 116, B08206.
Bryan, S.E., Ewart, A., Stephens, C.J., Parianos, J., Downes, P.J., 2000. The Whitsunday Volcanic Province, Central Queensland, Australia: lithological and stratigraphic investigations of a silicic-dominated large igneous province. J. Volcanol. Geoth. Res. 99, 55–78.
Cannaò, E., Malaspina, N., 2018. From oceanic to continental subduction: implications for the geochemical and redox evolution of the supra-subduction mantle. Geosphere 14, 2311–2336.
Chang, J., Audétat, A., 2023a. Post-subduction porphyry Cu magmas in the Sanjiang region of southwestern China formed by fractionation of lithospheric mantle–derived mafic magmas. Geology 51, 64–68.
Chang, J., Audétat, A., 2023b. Experimental Equilibrium and fractional crystallization of a H_2O, CO_2, Cl and S-bearing potassic mafic magma at 1.0 GPa, with implications for the origin of porphyry Cu (Au, Mo)-forming potassic magmas. J. Petrol. 64, egad034.
Cloos, M., Sapiie, B., van Ufford, A.Q., Weiland, R.J., Warren, P.Q., McMahon, T.P., 2005. Collisional delamination in New Guinea: the geotectonics of subducting slab breakoff. Geol. Soc. Am. Spec. Pap. 400.
Condamine, P., Médard, E., Devidal, J.L., 2016. Experimental melting of phlogopite-peridotite in the garnet stability field. Contrib. Miner. Petrol. 171, 95.
Conticelli, S., Guarnieri, L., Farinelli, A., Mattei, M., Avanzinelli, R., Bianchini, G., Boari, E., Tommasini, S., Tiepolo, M., Prelevic, D., Venturelli, G., 2009. Trace elements and Sr–Nd–Pb isotopes of K-rich to shoshonitic, and calc-alkalic magmatism of the Western Mediterranean region: genesis of ultrapotassic to calc-alkaline magmatic associations in a post-collisional geodynamic setting. Lithos 107, 68–92.
Cooke, D.R., Hollings, P., Walshe, J.L., 2005. Giant porphyry deposits: characteristics, distribution, and tectonic controls. Econ. Geol. 100, 801–818.
Cottrell, E., Birner, S.K., Brounce, M., Davis, F.A., Waters, L.E., Kelley, K.A., 2021. Oxygen fugacity across tectonic settings. In: Moretti, R., Neuville, D.R. (Eds.), Magma Redox Geochemistry. Wiley, pp. 33–61.
Couzinié, S., Laurent, O., Moyen, J.F., Zeh, A., Bouilhol, P., Villaros, A., 2016. Post-collisional magmatism: crustal growth not identified by zircon Hf–O isotopes. Earth Planet. Sci. Lett. 456, 182–195.
Davies, H.L., 1980. Folded thrust fault and associated metamorphics in the Suckling-Dayman massif, Papua New Guinea. Am. J. Sci. 280A, 171–191.
Davies, H.L., 2012. The geology of New Guinea – the cordilleran margin of the Australian continent. Episodes 35, 87–102.
Davies, H.L., Warren, R.G., 1988. Origin of eclogite-bearing, domed, layered metamorphic complexes ("core complexes") in the D'Entrecasteaux islands, Papua New Guinea. Tectonics 7, 1–21.
Davies, H.L., Symonds, P.A., Ripper, I.D., 1984. Structure and evolution of the southern Solomon Sea region. BMR J. Aust. Geol. Geophys. 9, 49–68.
DesOrmeau, J.W., Gordon, S.M., Little, T.A., Bowring, S.A., Chatterjee, N., 2017. Rapid time scale of Earth's youngest known ultrahigh-pressure metamorphic event, Papua New Guinea. Geology 45, 795–798.
Ding, L., Kapp, P., Zhong, D., Deng, W., 2003. Cenozoic volcanism in Tibet: evidence for a transition from oceanic to continental subduction. J. Petrol. 44, 1833–1865.
Dugmore, M.A., Leaman, P.W., Philip, R., 1996. Discovery of the Mt Bini porphyry copper-gold-molybdenum deposit in the Owen Stanley Ranges, Papua New Guinea—a geochemical case history. J. Geochem. Explor. 57, 89–100.
Eilon, Z., Abers, G.A., Gaherty, J.B., Jin, G., 2015. Imaging continental breakup using teleseismic body waves: the Woodlark Rift, Papua New Guinea. Geochem. Geophys. Geosyst. 16, 2529–2548.
Ewart, A., Schon, R.W., Chappell, B.W., 1992. The Cretaceous volcanic-plutonic province of the central Queensland (Australia) coast—a rift related 'calc-alkaline' province. Earth Environ. Sci. Trans. R. Soc. Edinb. 83, 327–345.
Feldstein, S.N., Lange, R.A., 1999. Pliocene potassic magmas from the Kings River region, Sierra Nevada, California: evidence for melting of a subduction-modified mantle. J. Petrol. 40, 1301–1320.
Foley, S.F., 1985. The oxidation state of lamproitic magmas. Tscher. Miner. Petrog. Mitteilungen 34, 217–238.
Foley, S.F., 1992. Vein-plus-wall-rock melting mechanisms in the lithosphere and the origin of potassic alkaline magmas. Lithos 28, 435–453.
Foley, S., Venturelli, G., Green, D.H., Toscani, L., 1987. The ultrapotassic rocks: characteristics, classification, and constraints for petrogenetic models. Earth Sci. Rev. 24, 81–134.
Franz, L., Romer, R.L., de Capitani, C., 2013. Protoliths and phase petrology of whiteschists. Contrib. Miner. Petrol. 166, 255–274.
Green, D.H., 1961. Ultramafic breccias from the Musa Valley, eastern Papua. Geol. Mag. 98, 1–26.
Grondahl, C., Zajacz, Z., 2017. Magmatic controls on the genesis of porphyry Cu–Mo–Au deposits: the Bingham Canyon example. Earth Planet. Sci. Lett. 480, 53–65.
Gülmez, F., Prelević, D., Förster, M.W., Buhre, S., Günther, J., 2023. Experimental production of K-rich metasomes through sediment recycling at the slab-mantle interface in the fore-arc. Sci. Rep. 13, 19608.
Hamilton, P.J., Johnson, R.W., Mackenzie, D.E., O'nions, R.K., 1983. Pleistocene volcanic rocks from the Fly-Highlands province of western Papua New Guinea: a note on new Sr and Nd isotopic data and their petrogenetic implications. J. Volcanol. Geoth. Res. 18, 449–459.
Hegner, E., Smith, I.E., 1992. Isotopic compositions of late Cenozoic volcanics from southeast Papua New Guinea: evidence for multi-component sources in arc and rift environments. Chem. Geol. 97, 233–249.
Hermann, J., Rubatto, D., 2009. Accessory phase control on the trace element signature of sediment melts in subduction zones. Chem. Geol. 265, 512–526.
Hill, K.C., Hall, R., 2003. Mesozoic–Cenozoic evolution of Australia's New Guinea margin in a west Pacific context. In: Hillis, R.R., Müller, R.D. (Eds.), Evolution and dynamics of the Australian Plate. Geol. Soc. Australia Spec. Publ. 22 and Geol. Soc. America Spec. Pap. 372, pp. 265–289. https://doi.org/10.1130/0-8137-2372-8.265.
Hill, K.C., Kendrick, R.D., Crowhurst, P.V., Gow, P.A., 2002. Copper-gold mineralisation in New Guinea: tectonics, lineaments, thermochronology and structure. Aust. J. Earth Sci. 49, 737–752.
Hill, K.C., Raza, A., 1999. Arc–continent collision in Papua Guinea: constraints from fission track thermochronology. Tectonics 18, 950–966.
Holm, R.J., Spandler, C., Richards, S.W., 2015. Continental collision, orogenesis and arc magmatism of the Miocene Maramuni arc, Papua New Guinea. Gondwana Res. 28, 1117–1136.
Holm, R.J., Rosenbaum, G., Richards, S.W., 2016. Post 8 Ma reconstruction of Papua New Guinea and Solomon Islands: microplate tectonics in a convergent plate boundary setting. Earth Sci. Rev. 156, 66–81.
Holm, R.J., Tapster, S., Jelsma, H.A., Rosenbaum, G., Mark, D.F., 2019. Tectonic evolution and copper-gold metallogenesis of the Papua New Guinea and Solomon Islands region. Ore Geol. Rev. 104, 208–226.
Holwell, D.A., Fiorentini, M., McDonald, I., Lu, Y., Giuliani, A., Smith, D.J., Keith, M., Locmelis, M., 2019. A metasomatized lithospheric mantle control on the metallogenic signature of post-subduction magmatism. Nat. Commun. 10, 3511.
Hou, Z., Yang, Z., Qu, X., Meng, X., Li, Z., Beaudoin, G., Rui, Z., Gao, Y., Zaw, K., 2009. The Miocene Gangdese porphyry copper belt generated during post-collisional extension in the Tibetan Orogen. Ore Geol. Rev. 36, 25–51.
Hou, Z., Duan, L., Lu, Y., Zheng, Y., Zhu, D., Yang, Z., Yang, Z., Wang, B., Pei, Y., Zhao, Z., McCuaig, T.C., 2015a. Lithospheric architecture of the Lhasa Terrane and its control on ore deposits in the Himalayan-Tibetan Orogen. Econ. Geol. 110, 1541–1575.
Hou, Z., Yang, Z., Lu, Y., Kemp, A., Zheng, Y., Li, Q., Tang, J., Yang, Z., Duan, L., 2015b. A genetic linkage between subduction-and collision-related porphyry Cu deposits in continental collision zones. Geology 43, 247–250.
Housh, T., McMahon, T.P., 2000. Ancient isotopic characteristics of Neogene potassic magmatism in Western New Guinea (Irian Jaya, Indonesia). Lithos 50, 217–239.
Jin, G., Gaherty, J.B., Abers, G.A., Kim, Y., Eilon, Z., Buck, W.R., 2015. Crust and upper mantle structure associated with extension in the Woodlark Rift, Papua New Guinea from Rayleigh-wave tomography. Geochem. Geophys. Geosyst. 16, 3808–3824.
Johnson, R.W., Mackenzie, D.E., Smith, I.E.M., 1978. Delayed partial melting of subduction-modified mantle in Papua New Guinea. Tectonophysics 46, 197–216.
Large, S.J.E., Quadt, A., von Wotzlaw, J.-F., Guillong, M., Heinrich, C.A., 2018. Magma evolution leading to porphyry Au–Cu mineralization at the Ok Tedi deposit, Papua New Guinea: trace element geochemistry and high-precision geochronology of igneous zircon. Econ. Geol. 113, 39–61.
Li, W., Yang, Z., Chiaradia, M., Lai, Y., Yu, C., Zhang, J., 2020. Redox state of southern Tibetan upper mantle and ultrapotassic magmas. Geology 48, 733–736.
Little, T.A., Webber, S.M., Mizera, M., Boulton, C., Oesterle, J., Ellis, S., Boles, A., van der Pluijm, B., Norton, K., Seward, D., Biemiller, J., Wallace, L., 2019. Evolution of a rapidly slipping, active low-angle normal fault, Suckling-Dayman metamorphic core complex, SE Papua New Guinea. Geol. Soc. Am. Bull. 131, 1333–1363.
Luo, C.H., Wang, R., Weinberg, R.F., Hou, Z., 2022. Isotopic spatial-temporal evolution of magmatic rocks in the Gangdese belt: implications for the origin of Miocene post-collisional giant porphyry deposits in southern Tibet. Geol. Soc. Am. Bull. 134, 316–324.
Mackenzie, D.E., 1976. Nature and origin of late Cenozoic volcanoes in western Papua New Guinea. In: Johnson, R.W. (Ed.), Volcanism in Australasia. Elsevier Sci., Amsterdam, pp. 221–238.
Mallik, A., Nelson, J., Dasgupta, R., 2015. Partial melting of fertile peridotite fluxed by hydrous rhyolitic melt at 2–3 GPa: implications for mantle wedge hybridization by sediment melt and generation of ultrapotassic magmas in convergent margins. Contrib. Miner. Petrol. 169, 48.
McMahon, T.P., 1994. Pliocene intrusions in the Gunung Bijih (Ertsberg) mining district, Irian Jaya, Indonesia: major-and trace-element chemistry. Int. Geol. Rev. 36, 925–946.
McMahon, T.P., 2001. Origin of a collision-related ultrapotassic to calc-alkaline magmatic suite: the latest Miocene Minjauh volcanic field, Irian Jaya, Indonesia. Bull. Geol. Jurusan Teknik Geol. Inst. Teknol. Bandung 33, 47–77.
Miller, C.H., Schuster, R., Klötzli, U., Frank, W., Purtscheller, F., 1999. Post-collisional potassic and ultrapotassic magmatism in SW Tibet: geochemical and Sr–Nd–Pb–O isotopic constraints for mantle source characteristics and petrogenesis. J. Petrol. 40, 1399–1424.
Misztela, M.A., Campbell, I.H., Arculus, R.J., 2022. Platinum-group element geochemistry and magma evolution of the Mount Hagen (Papua New Guinea) magmatic system. J. Petrol. 63, 1–20.
Moyen, J.F., Laurent, O., Chelle-Michou, C., Couzinié, S., Vanderhaeghe, O., Zeh, A., Villaros, A., Gardien, V., 2017. Collision vs. subduction-related magmatism: two

contrasting ways of granite formation and implications for crustal growth. Lithos 277, 154–177.
Mullen, E.K., McCallum, I.S., 2013. Coexisting pseudobrookite, ilmenite, and titanomagnetite in hornblende andesite of the Coleman Pinnacle flow, Mount Baker, Washington: evidence for a highly oxidized arc magma. Am. Mineral. 98, 417–425.
Müller, D., Groves, D.I., 1993. Direct and indirect associations between potassic igneous rocks, shoshonites and gold–copper deposits. Ore Geol. Rev. 8, 383–406.
Mungall, J.E., 2002. Roasting the mantle: Slab melting and the genesis of major Au and Au-rich Cu deposits. Geology 30, 915–918.
Nandedkar, R.H., Hürlimann, N., Ulmer, P., Müntener, O., 2016. Amphibole–melt trace element partitioning of fractionating calc-alkaline magmas in the lower crust: an experimental study. Contrib. Miner. Petrol. 171, 71.
Österle, J.E., Little, T.A., Seward, D., Stockli, D.F., Gamble, J., 2020. The petrology, geochronology and tectono-magmatic setting of igneous rocks in the Suckling-Dayman metamorphic core complex, Papua New Guinea. Gondwana Res. 83, 390–414.
Pang, K.N., Chung, S.L., Zarrinkoub, M.H., Wang, F., Kamenetsky, V.S., Lee, H.Y., 2015. Quaternary high-Mg ultrapotassic rocks from the Qal'eh Hasan Ali maars, southeastern Iran: petrogenesis and geodynamic implications. Contrib. Miner. Petrol. 170, 1–19.
Park, J.W., Campbell, I.H., Chiaradia, M., Hao, H., Lee, C.T., 2021. Crustal magmatic controls on the formation of porphyry copper deposits. Nat. Rev. Earth Environ. 2, 542–557.
Park, S.H., Michael, P.J., Kamenov, G.D., Lee, S.M., Hauff, F., Lee, K.Y., 2018. Petrogenesis of basalts along the eastern Woodlark spreading center, equatorial western Pacific. Lithos 316–317, 122–136.
Peccerillo, A., 1999. Multiple mantle metasomatism in Central-Southern Italy: geochemical effects, timing and geodynamic implications. Geology 27, 315–318.
Pettke, T., Oberli, F., Heinrich, C.A., 2010. The magma and metal source of giant porphyry-type ore deposits, based on lead isotope microanalysis of individual fluid inclusions. Earth Planet. Sci. Lett. 296, 267–277.
Pieters, P.E., 1978. Port Moresby-Kalo-Aroa - Papua New Guinea, 1:250 000 geological series. Bur. Miner. Resour. Aust. Explanatory Notes, SC/55-6,7,11.
Pollard, P.J., Taylor, R.G., Peters, L., 2005. Ages of intrusion, alteration, and mineralization at the Grasberg Cu-Au deposit, Papua, Indonesia. Econ. Geol. 100, 1005–1020.
Pollard, P.J., Jongens, R., Stein, H., Mark Fanning, C., Smillie, R., 2021. Rapid formation of porphyry and skarn copper-gold mineralization in a postsubduction environment: Re–Os and U-Pb geochronology of the Ok Tedi Mine, Papua New Guinea. Econ. Geol. 116, 533–558.
Prelević, D., Foley, S.F., Romer, R., Conticelli, S., 2008. Mediterranean Tertiary lamproites derived from multiple source components in postcollisional geodynamics. Geochim. Cosmochim. Acta 72, 2125–2156.
Richards, J.P., 2009. Postsubduction porphyry Cu–Au and epithermal Au deposits: products of remelting of subduction-modified lithosphere. Geology 37, 247–250.
Richards, J.P., 2015a. Tectonic, magmatic, and metallogenic evolution of the Tethyan orogen: from subduction to collision. Ore Geol. Rev. 70, 323–345.
Richards, J.P., 2015b. The oxidation state, and sulfur and Cu contents of arc magmas: implications for metallogeny. Lithos 233, 27–45.
Richards, J.P., 2022. Porphyry copper deposit formation in arcs: what are the odds? Geosphere 18, 130–155.
Richards, J.P., Chappell, B.W., McCulloch, M.T., 1990. Intraplate-type magmatism in a continent-island-arc collision zone: Porgera intrusive complex, Papua New Guinea. Geology 18, 958–961.
Richards, J.P., Şengör, A.C., 2017. Did Paleo-Tethyan anoxia kill arc magma fertility for porphyry copper formation? Geology 45, 591–594.
Rielli, A., Tomkins, A.G., Nebel, O., Brugger, J., Etschmann, B., Evans, K.A., Wykes, J.L., Vasilyev, P., Paterson, D.J., 2022. Incipient metal and sulfur extraction during melting of metasomatised mantle. Earth Planet. Sci. Lett. 599, 117850.
Rock, N.M.S., Groves, D.I., 1988. Can lamprophyres resolve the genetic controversy over mesothermal gold deposits? Geology 16, 538–541.
Rock, N.M.S., Groves, D.I., Perring, C.S., Golding, S.D., 1989. Gold, lamprophyres, and porphyries: what does their association mean. Econ. Geol. Monogr. 6, 609–625.
Romer, R.L., Heinrich, W., Schröder-Smeibidl, B., Meixner, A., Fischer, C.O., Schulz, C., 2005. Elemental dispersion and stable isotope fractionation during reactive fluid-flow and fluid immiscibility in the Bufa del Diente aureole, NE-Mexico: evidence from radiographies and Li, B, Sr, Nd, and Pb isotope systematics. Contrib. Miner. Petrol. 149, 400–429.
Rosenbaum, G., 2018. The Tasmanides: phanerozoic tectonic evolution of eastern Australia. Annu. Rev. Earth Planet. Sci. 46, 291–325.
Schmidt, M.W., Vielzeuf, D., Auzanneau, E., 2004. Melting and dissolution of subducting crust at high pressures: the key role of white mica. Earth Planet. Sci. Lett. 228, 65–84.
Shafiei, B., Haschke, M., Shahabpour, J., 2009. Recycling of orogenic arc crust triggers porphyry Cu mineralization in Kerman Cenozoic arc rocks, southeastern Iran. Mineral. Deposita 44, 265–283.
Sillitoe, R.H., 2002. Some metallogenic features of gold and copper deposits related to alkaline rocks and consequences for exploration. Miner. Depos. 37, 4–13.
Sillitoe, R.H., 2010. Porphyry copper systems. Econ. Geol. 105, 3–41.
Smith, I.E.M., 1982. Volcanic evolution in eastern Papua. Tectonophysics 87, 333–365.
Smith, I.E.M., 2014. High-magnesium andesites: the example of the Papuan Volcanic Arc. Geol. Soc. (Lond.) Spec. Publ. 385, 117–135.
Soder, C.G., Romer, R.L., 2018. Post-collisional potassic–ultrapotassic magmatism of the Variscan orogen: implications for mantle metasomatism during continental subduction. J. Petrol. 59, 1007–1034.
Sun, W.D., Liang, H.Y., Ling, M.X., Zhan, M.Z., Ding, X., Zhang, H., Yang, X.Y., Li, Y.L., Ireland, T.R., Wei, Q.R., Fan, W.M., 2013. The link between reduced porphyry copper deposits and oxidized magmas. Geochim. Cosmochim. Acta 103, 263–275.
Taylor, G.A., 1958. The 1951 eruption of Mount Lamington, Papua. Aust. Bur. Miner. Resour. Geol. Geophys. Bull. 38, 1–117.
Taylor, B., Goodliffe, A.M., Martinez, F., 1999. How continents break up: insights from Papua New Guinea. J. Geophys. Res.: Solid Earth 104, 7497–7512.
van Dongen, M., Weinberg, R.F., Tomkins, A.G., Armstrong, R.A., Woodhead, J.D., 2010a. Recycling of Proterozoic crust in Pleistocene juvenile magma and rapid formation of the Ok Tedi porphyry Cu–Au deposit, Papua New Guinea. Lithos 114, 282–292.
van Dongen, M., Weinberg, R.F., Tomkins, A.G., 2010b. REE-Y, Ti, and P remobilization in magmatic rocks by hydrothermal alteration during Cu-Au deposit formation. Econ. Geol. 105, 763–776.
Wang, Z., Cheng, H., Zong, K., Geng, X., Liu, Y., Yang, J., Wu, F., Becker, H., Foley, S., Wang, C.Y., 2020. Metasomatized lithospheric mantle for Mesozoic giant gold deposits in the North China craton. Geology 48, 169–173.
Wang, R., Weinberg, R.F., Collins, W.J., Richards, J.P., Zhu, D.C., 2018. Origin of postcollisional magmas and formation of porphyry Cu deposits in southern Tibet. Earth Sci. Rev. 181, 122–143.
Xu, B., Griffin, W.L., Xiong, Q., Hou, Z.Q., O'Reilly, S.Y., Guo, Z., Pearson, N.J., Gréau, Y., Yang, Z.M., Zheng, Y.C., 2017. Ultrapotassic rocks and xenoliths from South Tibet: contrasting styles of interaction between lithospheric mantle and asthenosphere during continental collision. Geology 45, 51–54.
Zhang, D., Audétat, A., 2017. What caused the formation of the giant Bingham Canyon porphyry Cu-Mo-Au deposit? Insights from melt inclusions and magmatic sulfides. Econ. Geol. 112, 221–244.
Zhang, J., Davidson, J.P., Humphreys, M.C.S., Macpherson, C.G., Neill, I., 2015. Magmatic enclaves and andesitic lavas from Mt. Lamington, Papua New Guinea: implications for recycling of earlier-fractionated minerals through magma recharge. J. Petrol. 56, 2223–2256.
Zhao, Z., Mo, X., Dilek, Y., Niu, Y., DePaolo, D.J., Robinson, P., Zhu, D., Sun, C., Dong, G., Zhou, S., Luo, Z., Hou, Z., 2009. Geochemical and Sr–Nd–Pb–O isotopic compositions of the post-collisional ultrapotassic magmatism in SW Tibet: petrogenesis and implications for India intra-continental subduction beneath southern Tibet. Lithos 113, 190–212.
Zirakparvar, N.A., Baldwin, S.L., Vervoort, J.D., 2013. The origin and geochemical evolution of the Woodlark Rift of Papua New Guinea. Gondw. Res. 23, 931–943.